Molecular Motions in Fluctional Crystals: N-Base Adducts of Bis(1,5-cyclooctanediylboryl) Oxide

Mohamed Yalpani*[a], Roland Köster[a], and Roland Boese[b]

Max-Planck-Institut für Kohlenforschung[a],
Kaiser-Wilhelm-Platz 1, W-4330 Mülheim an der Ruhr

Institut für Anorganische Chemie der Universität Essen[b],
Universitätsstraße 5–7, W-4300 Essen

Received September 4, 1991

Key Words: Bis(1,5-cyclooctanediylboryl) oxide, N-base adducts of, solid state NMR of / Fluctional crystals / Crystal dynamics / Phase transformations

The adducts of bis(1,5-cyclooctanediylboryl) oxide (**1**) with quinuclidine (**2a**) and with pyridine (**2b**) show an unusually large premelting endothermic phase transition. **2a** has been investigated by ^{11}B-NMR spectroscopy in the solid state and at various temperatures in its mesophase. The significant differences in the lattice packings of the molecules of the thermally stable adducts of **1** with 4-methyl-, 3-bromo-, and 4-(dimethylamino)pyridine (**2c–e**; X-ray structural analysis) from those of **2a** and **2b** suggests that it is the unique molecular arrangement in the respective lattices of the latter two adducts which allows a smooth transition to a two-dimensionally ordered mesophase. This is stabilized by intermolecular fluctuation of the N-base molecules between the boron atoms of the neighbouring molecules of **1**.

In an earlier publication[1] we described an unusual thermal solid-state phenomenon of the (1:1) adducts of bis(1,5-cyclooctanediylboryl)oxide (**1**) with the N-bases quinuclidine (**Q**) and pyridine (**P**) (**2a, b**).

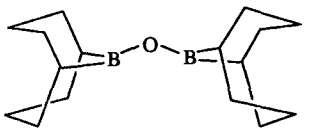

1

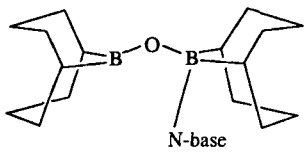

2

No.	N-base
2a	quinuclidine
2b	pyridine
2c	4-methylpyridine
2d	3-bromopyridine
2e	4-(dimethylamino)-pyridine

Only these two of a number of such adducts show a relatively large premelting endothermic transformation in their DSC thermograms[1]. These phase transitions can also be observed when viewed under a microscope. At above 90 and 120 °C, crystals of **2a** and **2b**, respectively, transform to an opaque and waxy looking material very similar to that familiar in plastic crystals.

However, the structural features of these compounds are incompatible with those attributed to this class of compounds[2]. Based on the observed unique pairing of molecules of **2a** and **2b** in their crystal cells (see Figure 1, **2a, b**) we proposed a novel type of mesophase in which the N-base molecules fluctuate between the boron atoms of neighbouring acceptor molecules. It has been suggested that this to-and-fro motion would maintain a measure of order throughout the assembly as in the mesophases of liquid crystals. We provisionally referred to this new state as fluctional crystalline phase[1].

In this communication we present further experimental evidence in support of this proposal.

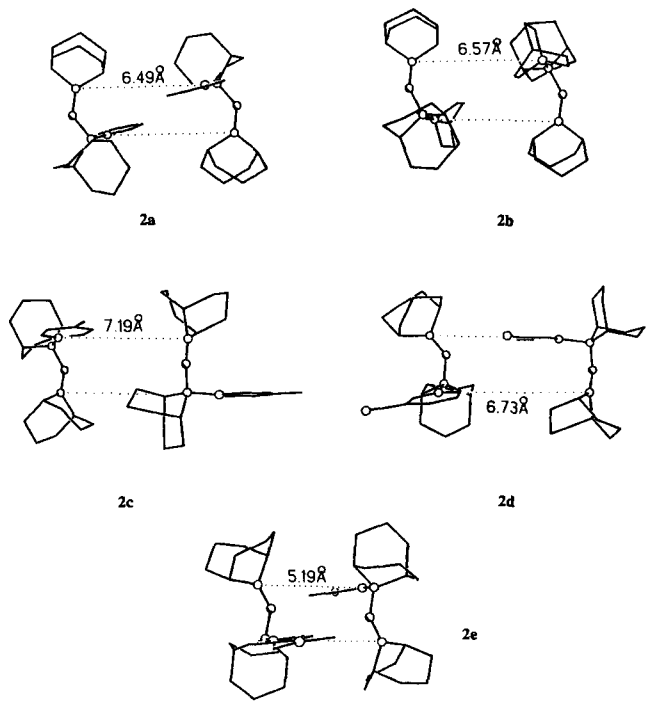

Fig. 1. Pairing of the molecules of **2a–2e** in their respective lattices. (Dotted lines designate the non-bonded intermolecular B...N′ distances)

  0009–2940/92/0202–0309 $ 3.50+.25/0

Result and Discussion

It was anticipated that information on the nature of the order-mesophase transitions and on the prevailing "ordered" molecular motion in **2a** and **2b** at higher temperatures could be obtained by measuring NMR spectra of these compounds in their mesophases. Since even in solution the ^{13}C-NMR spectra of these compounds had revealed only small chemical shift differences[1] it was anticipated that the technique of CP-MAS would yield little information in these cases. Simple high-resolution NMR techniques have been applied in the past in ^{1}H- and ^{13}C-NMR studies involving plastic[3] and liquid crystals[4] and meaningful spectra have been obtained. For our investigations the presence of two types of boron atoms with widely separated ^{11}B-NMR signals ($\delta \approx 55$ for the trigonal and $\delta \approx 0-10$ for the tetragonal boron atoms) promised to provide a sensitive probe.

Utilizing the described procedure[3] we prepared a homogeneous sample by first melting the crystalline **2a** and **2b** in a 5-mm NMR tube at 140°C. These samples, after having been once cooled to −78°C, were used for the NMR experiments described below.

For **2a** at room temperature and significantly below 75°C only a broad peak centred at $\delta \approx 54$ ($h_{1/2} \approx 2000$ Hz $\triangleq$ 30 ppm) is observed. The spectrum at 75°C (above the onset temperature of the first, smaller, endothermic phase transformation)[1] shows a relatively sharp signal (see Figure 2, a) at $\delta^{11}B = 56$ ($h_{1/2} = 700$ Hz). The very broad peak at about $\delta = 5$ ppm has only a minor integral intensity. A temperature rise to 85°C results in the spectrum shown in Figure 2, b. The developing shoulder to the peak at $\delta = 53$ is also very broad ($h_{1/2} = 4000$ Hz). At 90°C the spectrum (Figure 2, c) is drastically changed and only a broad signal at $\delta = 30$ ppm ($h_{1/2} = 4000$ Hz) is observed. A further increase of the temperature to 105°C causes a narrowing ($h_{1/2} = 3000$ Hz) and a slight shift of the signal to $\delta = 33$ ppm. A small shoulder at about $\delta = 55$ ppm is visible in Figure 2, d.

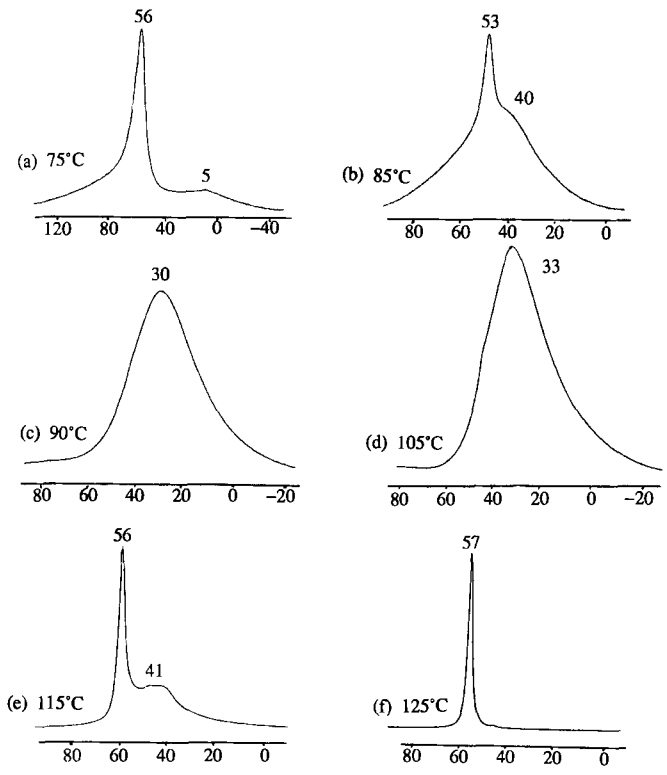

Fig. 2. ^{11}B-NMR (64.2 MHz) signals of solid and "solid" **2a** at various temperatures (values at peak apices are chemical shifts in ppm)

Another significant change is observed in the spectrum obtained at 115°C (Figure 2, e). The sharp peak at $\delta = 56$ ppm ($h_{1/2} = 400$ Hz) has a 1:1 integral intensity relative to the broad peak at about $\delta = 41$ ppm ($h_{1/2} = 2000$ Hz). A further rise in temperature of 5°C results only in an increase of this ratio. Finally at 125°C, the onset temperature for the clearing point, a single very narrow signal at $\delta = 57$ ($h_{1/2} = 250$ Hz) can be observed (Figure 3, f).

The "solid" state ^{11}B-NMR spectra of **2a**, measured at 75−125°C as depicted in Figures 2, a−f, show that major molecular changes occur in this temperature range. To some extent these spectral changes concur with the phase changes as indicated in the DSC thermogram of **2a**[1].

It should be noted that in these isothermal NMR experiments, complete transitions can be expected at the onset temperatures. Furthermore, due to the nature of the sample (a massive solid formed from the melt) the presence of non-crystalline zones (supercooled liquid pockets) is to be expected. In these zones molecular motions may prevail at temperatures well below the onset of the first phase transition. The very broad signal ($h_{1/2} = 4000$ Hz) observed in the spectra below 75°C are assigned to very restricted motion of molecules of **1** trapped in these zones. The significantly higher signal-to-noise ratio observed in the spectra obtained at these lower temperatures (despite running an equal number of scans) show that a large part of the sample which is present as a crystalline solid does not contribute to the observed signal intensity. In agreement with this only background noise was registered when an attempt was made to obtain a spectrum of a very densely packed pulverized crystalline sample of **2a**.

It can therefore be concluded that spectra obtained from solid **2a** below the first phase transition reveal only small degrees of molecular mobility. The passage past the onset of the first transition gives mainly rise to a very narrow single signal at $\delta \approx 56$ ppm, a value close to that commonly observed for uncomplexed **1**[5,6]. Such a spectrum can only result if both boron atoms in **2a** are chemically equivalent and both unassociated, or if one of the boron atoms experiences little rotational restriction while the second base-bound boron atom is rigidly held in the crystal lattice and therefore gives rise to a very broad signal. At a slightly higher temperature (85°C), yet below the main phase transition, two signals are observed (Figure 2, b). The peak at $\delta = 53$ can unquestionably be assigned to a trivalent boron atom (bound to an oxygen atom) in a dynamic environment. The broad peak centred at about $\delta = 40$ cannot a priori be assigned to a tetravalent boron atom.

However, information obtained from both the solid-state (X-ray diffraction[1]) and from solution ^{11}B- and ^{13}C-NMR[5]

spectra suggest that because of the severe intramolecular steric interactions, prevailing between the **Q** moiety and the large molecular skeleton of **1**, the N–B bond can adopt variable bond lengths and strengths at different temperatures. It can be surmised that in solid **2a** at 85 °C the motion of the (NB)-bound 9-borabicyclo[3.3.1]nonane ring increases, without completely interrupting the N–B bond and results in a broad signal at $\delta \approx 40$ ppm. A further rise in temperature to 90 °C brings about a coalescence of the molecular assembly. The ^{11}B-NMR signal at $\delta = 30$ indicates a rapid fluctuation of the N atom of **Q** between the boron atoms of **1**.

The spectrum depicted in Figure 2, c does not allow a differentiation to be made between an intra- or intermolecular to-and-fro motion. The special nature of the "solid" phase, however, favours an intermolecular dynamics. This condition should prevail throughout the temperature range (≈90 to 120 °C) of the mesophase. However, as the temperature is raised, the dominant intramolecular steric interactions result in the formation of non-degenerate equilibrium mixtures consisting of completely dissociated molecules of **Q** and **1**, and a weakly associated still fluctuating assemblage. The gradual decrease of signal intensity of $\delta \approx 43$ (Figure 2, e) at higher temperatures demonstrates the progressive shift of this equilibrium. Some of the stages of these stepwise transformations are schematized in Figure 3.

The above procedure has proved unsuitable for the investigation of the mesophase of **2b**. The DSC analysis has shown that its narrow mesophase (127–138 °C) is unstable. At very slow scanning rates (2 °C/min) the mesophase of **2b**

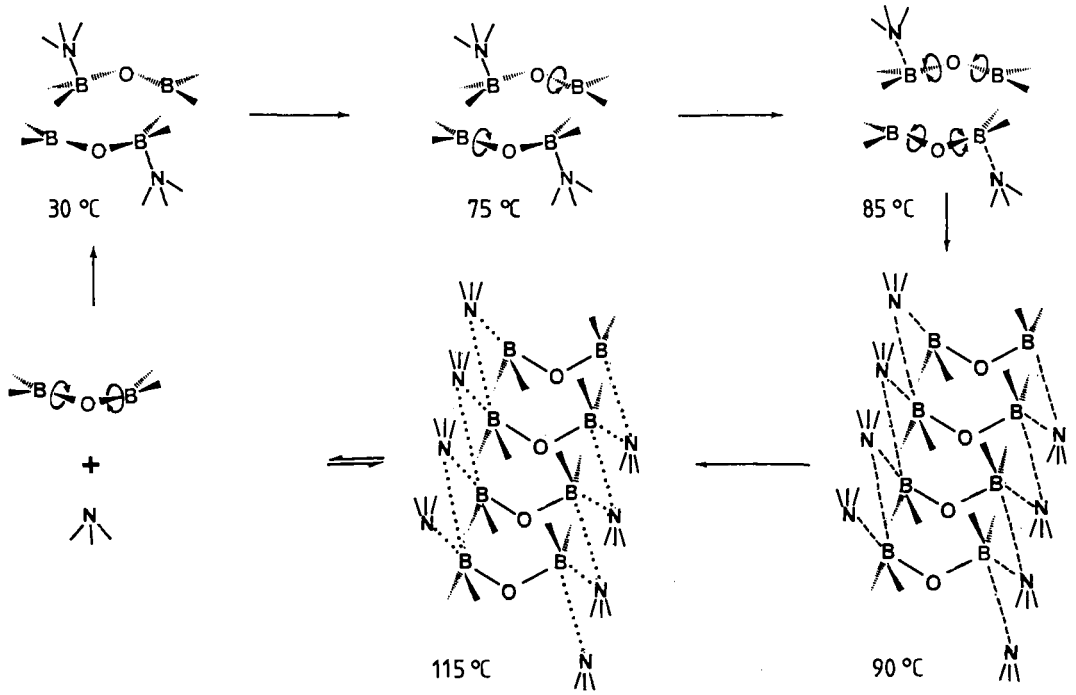

Fig. 3. Proposed stepwise transformation of molecules of **2a** with increasing temperature

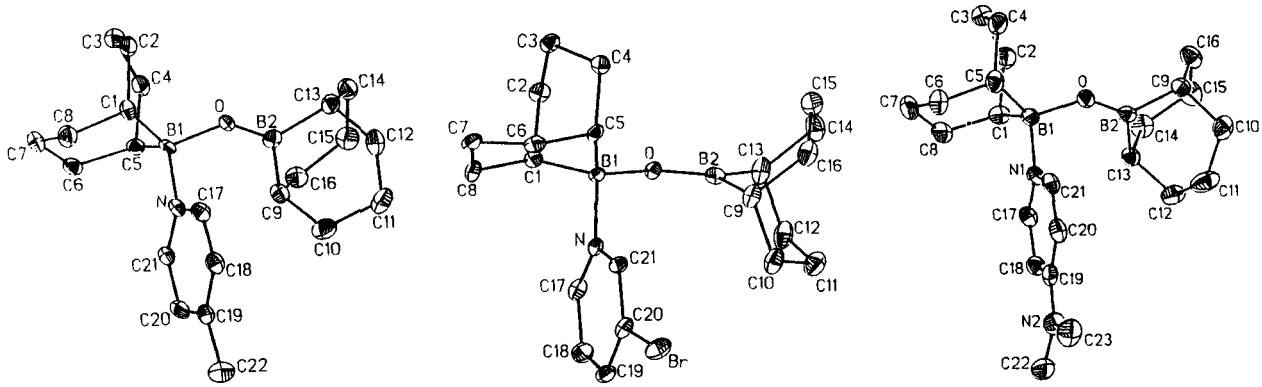

Fig. 4. Molecular structures of adducts **2c**–**2e**

can no longer be observed. Spectra have been obtained at 130°C and at 145°C ($\delta^{11}B \approx 58$). Presumably, when **2b** is held at, or above its melting point for a prolonged period, it slowly transforms into a clear liquid in which complete dissociation of the adduct into the components **P** and **1** is indicated.

A final question of interest was why only **2a** and **2b** among a number of sructurally similar adducts showed this unusual thermal behaviour. We expected to find an answer in subtle differences in the lattice structures of **2a** and **2b**[1] as compared to those of the thermally stable adducts. We therefore determined the crystal structures of the adducts of **1** with those of 4-methyl-, 3-bromo, and 4-(dimethylamino)pyridine adducts (**2c–e**) which were chosen amongst a large number of thermally inactive solid adducts of **1** (the choice was fortituous depending on the crystal quality of the available adducts).

The molecular structures found are depicted in Figure 4 and selected bond lengths and angles are listed in Table 1. All three structures basically resemble those of **2a** and **2b**[1].

Table 1. Selected bond lengths and angles for compounds **2c–2e**

Bond length (Å)				Bond angles (°)			
Bond	2c	2d	2e	Angle	2c	2d	2e
B1O	1.488 (3)	1.478 (5)	1.495 (2)	B1OB2	129.6 (2)	135.5 (3)	130.9 (1)
N1B1	1.643 (3)	1.674 (5)	1.635 (2)	NB1O	103.7 (2)	103.1 (3)	103.4 (1)
OB2	1.346 (3)	1.328 (5)	1.332 (2)	OB1C1	110.3 (2)	110.9 (3)	116.5 (1)
B1C1	1.613 (3)	1.612 (5)	1.619 (3)	OB1C5	113.5 (2)	116.9 (3)	108.8 (1)
B1C5	1.612 (3)	1.617 (6)	1.614 (3)	OB2C9	127.9 (2)	129.1 (4)	121.4 (1)
B2C9	1.585 (3)	1.608 (6)	1.586 (3)	OB2C13	121.5 (2)	120.5 (4)	128.3 (2)
B2CB	1.577 (3)	1.580 (6)	1.589 (2)				

Table 2. Crystallographic data for compounds **2c–2e** and data collection procedures

	2c	2d	2e
Formula	$C_{21}H_{35}B_2NO$	$C_{21}H_{32}B_2BrNO$	$C_{23}H_{38}B_2N_2O$
Crystal Size (mm)	0.38x0.25x0.19	0.40x0.34x0.28	0.51x0.43x0.38
Space group	$P2_1/n$	$P2_12_12_1$	C2/c
Z	4	4	8
a (Å)	7.074 (1)	10.874 (2)	20.346 (4)
b (Å)	16.015 (2)	11.116 (1)	11.628 (3)
c (Å)	17.764 (2)	16.547 (2)	18.268 (4)
α (deg)	90	90	90
β (deg)	96.64 (1)	90	91.48 (2)
γ (deg)	90	90	90
T (K)	120	120	125
V (Å^3)	1999.0 (4)	2009.6 (4)	4320.4 (1.5)
d_{calc} (g/cm^3)	1.207	1.375	1.16
μ (mm^{-1})	0.07	2.06	0.06
Radiation	Mo-K_α	Mo-K_α	Mo-K_α
$2\Theta_{max}$ (deg)	45	50	55
Total no. of unique reflections	2359	3563	4402
Observed reflections	2028	3226	3647
R	0.0447	0.0388	0.053
R_w [$w=\sigma^2(F_o)+gF^2$]	0.0497	0.0404	0.058
g	5.0×10^{-4}	1.61×10^{-3}	2.41×10^{-4}
Residual electron density (e/Å^3)	0.237	0.78	0.56

One interesting feature is the unusual boat-chair conformation of one of the 9-borabicyclo[3.3.1]nonane skeletons (ring incorporating B2) in **2d** and **2e** (another example of crystallization of a 9-borabicyclo[3.3.1]nonane skeleton in this conformation was reported earlier[5]).

The significant difference between the thermally active crystalline adducts **2a** and **2b** and other thermally stable adducts of **1** becomes evident in the packing of the respective molecules in their cell. All adducts appear to crystallize in head-to-tail configurated pairs. In both **2a** and **2b** the oxygen atoms are situated on the periphery of the molecular pairs (see Figure 1, a and b). In **2c** and **2d** the N-base moiety is located between the pair (see Figure 1, c and d) and in **2e** the oxygen atoms of the **1** moieties point towards each other (see Figure 1, c). We believe that in **2c** and **2d** the unfavourable configuration of one of the base molecules and in **2e** the disadvantageous conformation of the nonbonding lone pair electrons of the opposing oxygen atoms have the wrong topology for the initiation of the intermolecular fluctuation. This leads to the conclusion that the fluctuation observed in "solid" **2a** and **2b** is a fortuitous result of the molecular packing. It is interesting to note that for **2b** the reheat DSC scan does not reproduce the virgin run result[1]. It seems probable that in the crystalline mass of **2b**, obtained from the melt, a molecular packing similar to those observed for **2c** and **2d**, or **2e** is present.

Table 3. Atomic coordinates (× 10^4) and equivalent isotropic displacement factors [Å^2 × 10^3] for **2c**

	x	y	z	U_{eq}
B(1)	7376(4)	918(2)	6571(1)	17(1)*
B(2)	6663(4)	718(2)	7943(2)	19(1)*
O	6194(2)	713(1)	7187(1)	17(1)*
N	8978(3)	171(1)	6628(1)	17(1)*
C(1)	6106(3)	875(1)	5757(1)	19(1)*
C(2)	4449(3)	1491(2)	5777(1)	24(1)*
C(3)	4983(3)	2382(2)	6039(1)	26(1)*
C(4)	6562(3)	2434(1)	6700(1)	22(1)*
C(5)	8257(3)	1847(1)	6634(1)	19(1)*
C(6)	9342(3)	2087(1)	5957(1)	21(1)*
C(7)	8349(3)	1880(2)	5169(1)	26(1)*
C(8)	7331(4)	1039(2)	5117(1)	25(1)*
C(9)	8719(4)	799(1)	8396(1)	22(1)*
C(10)	9162(3)	-66(2)	8758(1)	29(1)*
C(11)	7660(4)	-401(2)	9235(1)	30(1)*
C(12)	5616(4)	-308(2)	8864(1)	27(1)*
C(13)	5133(3)	555(1)	8505(1)	21(1)*
C(14)	5177(3)	1277(1)	9080(1)	24(1)*
C(15)	7139(4)	1502(2)	9480(1)	26(1)*
C(16)	8719(3)	1527(2)	8967(1)	26(1)*
C(17)	8377(3)	-623(1)	6542(1)	21(1)*
C(18)	9582(3)	-1290(1)	6648(1)	21(1)*
C(19)	11522(3)	-1164(1)	6847(1)	21(1)*
C(20)	12139(3)	-346(1)	6910(1)	21(1)*
C(21)	10846(3)	297(1)	6809(1)	17(1)*
C(22)	12883(4)	-1880(2)	6985(1)	31(1)*

* Equivalent isotropic U defined as one third of the trace of the orthogonalized U_{ij} tensor.

We are grateful to Prof. *B. Wrackmeyer* and Dr. *W. V. Dahlhoff* for valuable discussions on the subject of this manuscript and to Mr. *W. Wisniewski* for measurements of the solid-state ^{11}B-NMR spectra.

Experimental

The synthesis of the 1:1 N-base adducts **2a**–**2e**, the DSC and the X-ray structural analysis of **2a** and **2b** were reported earlier[1,6]. Data collection and calculations for the adducts **2c**–**2e** were carried out on a Nicolet R3m/V four-cycle diffractometer with Microvax II and SHELXTL-PLUS software[7]. After empirical absorption corrections for **2d**, the structure solutions were performed by direct methods and for refinements all hydrogen atoms were included as rigid groups (C–H bond lengths at 0.96 Å, C–C–H and H–C–H angles at 109.5 and 120°, respectively). The isotropic displacement parameters of all the H atoms were refined in groups without constraints. Structural data on **2c**–**2e** are listed in Table 2 and the atomic coordinates in Tables 3–5 respectively[8]. For **2d** the absolute structure was established by refinement of η = 1.08(2)[9].

For the ^{11}B-NMR experiment, the sample was prepared by filling a standard 5-mm NMR tube with solid **2a**, sealed, heated to melt at 140°C, slowly cooled to room temperature and finally in a dry ice bath to −78°C. NMR measurements were carried out by continuous heating of the sample in a Bruker AC 200 spectrometer (diethyl ether–BF_3 as external standard). Before each data acquisition, by allowing a lapse of about 10 min, temperature equilibrium was reached.

Table 4. Atomic coordinates (× 10^4) and isotropic displacement factors [Å^2 × 10^3] for **2d** (definition of U as in Table 3)

	x	y	z	U_{eq}
Br	893(1)	6661(1)	1164(1)	23(1)*
B(1)	1884(4)	1918(3)	1287(3)	12(1)*
B(2)	3130(4)	2390(4)	2588(3)	17(1)*
N	874(3)	3029(3)	1430(2)	12(1)*
O	2422(2)	1747(3)	2099(2)	14(1)*
C(1)	1164(3)	732(3)	998(2)	14(1)*
C(2)	2136(4)	-276(3)	940(3)	17(1)*
C(3)	3220(3)	-15(3)	391(2)	17(1)*
C(4)	3772(3)	1238(3)	512(2)	14(1)*
C(5)	2824(3)	2262(3)	566(2)	15(1)*
C(6)	2130(4)	2473(4)	-233(2)	16(1)*
C(7)	1220(3)	1479(3)	-486(2)	18(1)*
C(8)	456(4)	943(4)	204(3)	18(1)*
C(9)	3584(4)	3753(4)	2492(3)	19(1)*
C(10)	2793(4)	4460(4)	3111(3)	25(1)*
C(11)	2948(4)	4009(4)	3978(3)	27(1)*
C(12)	2700(4)	2661(4)	4054(3)	26(1)*
C(13)	3480(4)	1906(4)	3456(2)	21(1)*
C(14)	4882(4)	2029(4)	3619(3)	27(1)*
C(15)	5545(4)	2642(4)	2925(3)	28(1)*
C(16)	4991(4)	3845(4)	2691(3)	24(1)*
C(17)	-186(4)	2811(4)	1810(2)	18(1)*
C(18)	-987(4)	3706(4)	2018(2)	20(1)*
C(19)	-714(4)	4889(4)	1836(2)	18(1)*
C(20)	383(4)	5098(3)	1437(2)	16(1)*
C(21)	1164(3)	4167(3)	1238(2)	14(1)*

Table 5. Atomic coordinates (× 10^4) and equivalent isotropic displacement factors [Å^2 × 10^3] for **2e** (definition of U as in Table 3)

	x	y	z	U_{eq}
O	3633(1)	2693(1)	4877(1)	227(4)*
N(1)	3400(1)	624(1)	4776(1)	213(4)*
N(2)	2744(1)	-2155(1)	6010(1)	327(5)*
B(1)	3641(1)	1751(2)	4320(1)	213(5)*
B(2)	3990(1)	2846(2)	5492(1)	220(5)*
C(1)	4334(1)	1521(2)	3928(1)	245(5)*
C(2)	4554(1)	2682(2)	3609(1)	330(6)*
C(3)	4064(1)	3227(2)	3068(1)	362(7)*
C(4)	3348(1)	3200(2)	3321(1)	354(6)*
C(5)	3122(1)	2060(2)	3667(1)	276(5)*
C(6)	3057(1)	1072(2)	3116(1)	344(6)*
C(7)	3702(1)	695(2)	2781(1)	364(6)*
C(8)	4274(1)	575(2)	3337(1)	319(6)*
C(9)	3892(1)	3941(1)	5994(1)	234(5)*
C(10)	3792(1)	3588(2)	6800(1)	338(6)*
C(11)	3848(1)	2311(2)	6924(1)	489(8)*
C(12)	4452(1)	1740(2)	6602(1)	353(6)*
C(13)	4580(1)	2081(2)	5806(1)	243(5)*
C(14)	5201(1)	2841(2)	5743(1)	319(6)*
C(15)	5146(1)	3999(2)	6129(1)	372(7)*
C(16)	4523(1)	4664(2)	5918(1)	327(6)*
C(17)	3800(1)	-254(1)	4970(1)	227(5)*
C(18)	3610(1)	-1170(2)	5381(1)	243(5)*
C(19)	2958(1)	-1242(2)	5623(1)	248(5)*
C(20)	2547(1)	-304(2)	5432(1)	266(5)*
C(21)	2780(1)	584(2)	5027(1)	243(5)*
C(22)	3177(1)	-3121(2)	6158(1)	368(6)*
C(23)	2071(1)	-2205(2)	6259(1)	429(7)*

CAS Registry Numbers

2a: 116996-19-1 / **2b**: 116972-69-1 / **2c**: 117497-84-4 / **2d**: 137846-40-3 / **2e**: 117497-87-7

[1] M. Yalpani, R. Köster, R. Boese, M. Sulkowski, *Chem. Ber.* **1989**, *122*, 9–17.

[2] Plastic crystals are characterized by the close to spherical mesogens which are able to attain rotational motion in the crystals without loosing positional order. In non-spherical molecules a disordered mesophase is thought to be the result of conformational motion within the molecules. In such a case a conformationally disordered (condis) crystal is said to be present: B. Wunderlich, M. Möller, H. G. Wiedemann, *Mol. Cryst. Liq. Cryst.* **1986**, *140*, 211–218.

[3] R. E. Pincock, K. R. Wilson, T. Kiovsky, *J. Am. Chem. Soc.* **1967**, *89*, 6890–6897.

[4] B. M. Fung, M. Gangoda, *J. Am. Chem. Soc.* **1985**, *107*, 3395–3396, and literature cited therein.

[5] M. Yalpani, R. Boese, R. Köster, *Chem. Ber.* **1990**, *123*, 1275–1283.

[6] M. Yalpani, J. Serwatowski, R. Köster, *Chem. Ber.* **1989**, *122*, 3–7.

[7] G. M. Sheldrick, *SHELXTL-PLUS (Version 2), an Integrated System for Solving, Refining, and Displaying Crystal Structures from Diffraction Data*, University of Göttingen, **1978**.

[8] Further details of the crystal structure investigations are available on request from the Fachinformationszentrum Karlsruhe, Gesellschaft für wissenschaftlich-technische Information mbH, W-7514 Eggenstein-Leopoldshafen 2, on quoting the depository numbers CSD-320379 (**2c**), -320380 (**2d**), -320381 (**2e**), the names of the authors, and the journal citation.

[9] D. Rogers, *Acta Crystallogr.* **1981**, *A37*, 734–741.

[341/91]